



Search for CP Violation in Semileptonic B_s Decays

The DØ Collaboration

URL: <http://www-d0.fnal.gov>

(Dated: July 25, 2008)

A search for CP violation in semileptonic B_s^0 decays was performed with a sample corresponding to approximately 2.8 fb^{-1} of integrated luminosity accumulated with the DØ Detector in Run II at the Fermilab Tevatron. The flavor of the final state of the B_s^0 meson was determined using the muon charge from the partially reconstructed decay $B_s^0 \rightarrow D_s^- \mu^+ \nu X$, $D_s^- \rightarrow \phi \pi^-$, $\phi \rightarrow K^+ K^-$. A combined tagging method was used for the initial-state flavor determination. The time-dependent fit to the distributions of B_s^0 candidates yields the CP violation parameter $a_{st}^s = -0.0024 \pm 0.0117(\text{stat})_{-0.0024}^{+0.0015}(\text{syst})$.

Preliminary Results for Summer 2008 Conferences

I. INTRODUCTION

At present, one of the most interesting topics in B physics is the measurement of CP violation (CPV) parameters in the $B_s^0 - \overline{B}_s^0$ system. The recent measurements at CDF and DØ show some deviation of the $B_s^0 - \overline{B}_s^0$ mixing phase ϕ_s from its Standard Model value. These measurements are based mainly on the analyses of decays $B_s^0 \rightarrow J/\psi\phi$ [1, 2] and inclusive di-muon analyses [3, 4]. Though $B_s^0 \rightarrow J/\psi\phi$ is considered as a “golden mode” for CP violation measurements, it requires a complicated angular analysis. The inclusive di-muon analysis depends heavily on b -fragmentation fractions and B_d^0 asymmetry results from the B factories. The analysis of semileptonic decays $B_s^0 \rightarrow X\mu^+D_s^-$ does not involve an angular analysis and is largely independent of the sample composition. Therefore it provides an important contribution to CP violation measurements. A time-integrated analysis of decays $B_s^0 \rightarrow X\mu^+D_s^-, D_s^- \rightarrow \phi\pi^-$ without initial-state flavor tagging was performed at DØ [5]. A more precise measurement can be obtained by using the information about initial-state flavor tagging and time dependence of the B decays. The corresponding technique was developed for the B_s^0 oscillation analysis [6]. The CPV analysis requires only some straightforward changes to the likelihood function and a study of detector asymmetries. The technique for extraction of detector asymmetries was developed for the inclusive di-muon analysis. It proved to be effective for the untagged time-integrated analysis and a similar approach can be used for the time-dependent analysis.

II. DETECTOR DESCRIPTION

The DØ detector is described in detail elsewhere [7, 8]. The following main elements of the DØ detector are essential for this analysis:

- The central-tracking system, which consists of a silicon microstrip tracker (SMT) and a central fiber tracker (CFT), both located within a 2-T superconducting solenoidal magnet;
- The liquid-argon/uranium calorimeter;
- The muon system located beyond the calorimeter.

The SMT has 800,000 individual strips, with typical pitch of 50 – 80 μm , and a design optimized for tracking and vertexing capability at $|\eta| < 3$, where $\eta = -\ln(\tan(\theta/2))$ and θ is the polar angle. The CFT has eight thin coaxial barrels, each supporting two doublets of overlapping scintillating fibers of 0.835 mm diameter, one doublet being parallel to the collision axis, and the other alternating by $\pm 3^\circ$ relative to the axis. The resolution of the impact parameter with respect to the collision point is about 20 μm for 5 GeV/ c tracks.

The three components of the liquid-argon/uranium calorimeter are housed in separate cryostats. A central section, lying outside the tracking system, covers up to $|\eta| = 1.1$. Two end calorimeters extend the coverage to $|\eta| \approx 4$.

The muon system consists of a layer of tracking detectors and scintillation trigger counters inside a 1.8 T iron toroid, followed by two additional layers outside the toroid. Tracking at $|\eta| < 1$ relies on 10 cm wide drift tubes, while 1-cm mini-drift tubes are used at $1 < |\eta| < 2$.

III. DATA SAMPLE

This analysis uses a sample of $B_s^0 \rightarrow D_s^- \mu^+ \nu X$, $D_s^- \rightarrow \phi\pi^-$, $\phi \rightarrow K^+K^-$ candidates selected with an offline filter from all data, representing 2.8 fb $^{-1}$ of proton-antiproton collisions, collected from April 2002 to September 2007 with no explicit trigger requirement, although most of the sample was collected by single muon triggers. The selections for the offline filter are described in [6]. The total number of D_s^- candidates passing the selection is 53,592 \pm 718 (stat.), while the number of D^- candidates is 14,499 \pm 341 (stat.) (see Fig. 1).

IV. FLAVOR TAGGING

A necessary step in the B_s^0 CPV analysis is the determination of the B_s^0/\overline{B}_s^0 final-state flavor. The presence of a muon in the B_s^0 semileptonic decay allows a determination of the final-state flavor since the b -quark flavor is correlated with the charge of the muon in the decays $B_s^0 \rightarrow \mu^+ X$ and $\overline{B}_s^0 \rightarrow \mu^- X$.

The initial-state flavor provides additional information that can be used in the likelihood. The initial-state flavor is determined using a combination of Opposite-Side [9] and Same-Side [10] tagging techniques. Each B candidate has an assigned d_{pr} variable, which gives a prediction of the dilution for that candidate. The calibration coefficients for the

dilution were determined using an Monte Carlo (MC) sample of $B_s^0 \rightarrow D_s^- \mu^+ \nu X$, $D_s^- \rightarrow \phi \pi^-$, $\phi \rightarrow K^+ K^-$ decays. The calibration was verified using reconstructed $B^\pm \rightarrow J/\psi K^\pm$ decays in data. The same technique was used for the measurement of the CP phase ϕ_s [1]. The B_s and B_d calibration is as follows:

$$\begin{aligned} \mathcal{D}(d_{pr}) \Big|_{d_{pr} < 0.6} &= 0.7895 \cdot |d_{pr}| + 0.3390 \cdot |d_{pr}|^2, \\ \mathcal{D}(d_{pr}) \Big|_{d_{pr} > 0.6} &= 0.6065. \end{aligned} \quad (1)$$

The B_u candidates are anticorrelated between Opposite-Side and Same-Side tagging and therefore a different formula was used:

$$\begin{aligned} \mathcal{D}(d_{pr}) \Big|_{d_{pr} < 0.45} &= 0, \\ \mathcal{D}(d_{pr}) \Big|_{d_{pr} > 0.45} &= 0.4393 \cdot |d_{pr}|. \end{aligned} \quad (2)$$

The efficiency of the combined tagging is close to 100%. In cases when the tagging information was not available the dilution was set to 0. Therefore the total sample used in the analysis corresponds to the sample presented in Fig. 1.

V. EXPERIMENTAL OBSERVABLES

The proper decay length of the B_s^0 meson, $c\tau_{B_s^0}$, for semileptonic decays can be written as

$$c\tau_{B_s^0} = x^M \cdot K, \quad \text{where } x^M = \frac{\mathbf{d}_T^B \cdot \mathbf{p}_T^{\mu D_s^-}}{(p_T^{\mu D_s^-})^2} \cdot cM_B. \quad (3)$$

x^M is the *visible proper decay length*, or VPDL, and K is the correction factor, also called the K factor. Semileptonic B decays necessarily have an undetected neutrino present in the decay chain, making a precise determination of the kinematics for the B meson impossible. In addition, other neutral or non-reconstructed charged particles can be present in the decay chain of the B meson. This leads to a bias towards smaller values of the B momentum, which is calculated using the reconstructed particles. A common practice to correct this bias is to scale the measured momentum of the B candidate by a K factor, which takes into account the effects of the neutrino and other lost or non-reconstructed particles. For this analysis, the K factor was defined as

$$K = p_T(\mu^+ D_s^-) / p_T(B_s^0), \quad (4)$$

where p_T denotes the absolute value of the transverse momentum. The K -factor distributions used to correct the data were obtained from the Monte Carlo simulation.

VI. FITTING PROCEDURE

All events with $1.72 < M(K^+ K^- \pi^-) < 2.22$ GeV/ c^2 were used in the unbinned likelihood fitting procedure. The likelihood for an event to arise from a specific source in the sample depends on the x^M , its uncertainty (σ_{x^M}), the mass of the D_s^- meson candidate (m), the predicted dilution (d_{pr}) and the selection variable y . All of the quantities used in the unbinned likelihood fitting procedure are known on an event-by-event basis. The *pdf* for each source can be expressed by the product of the corresponding *pdfs*:

$$f_i = P_i^{x^M}(x^M, \sigma_{x^M}, d_{pr}) P_i^{\sigma_{x^M}} P_i^m P_i^{d_{pr}} P_i^y. \quad (5)$$

The VPDL *pdf* $P_i^{x^M}(x^M, \sigma_{x^M}, d_{pr})$ represents a conditional probability, therefore it must be multiplied by $P_i^{\sigma_{x^M}}$ and $P_i^{d_{pr}}$ to have a joint *pdf* (see ‘‘Probability’’ section in PDG [17]). The *pdfs* P_i^m and P_i^y are used for separation of signal and background. The following sources, i , were considered:

- $\mu^+ D_s^- (\rightarrow \phi \pi^-)$ signal with fraction $\mathcal{F}_{\mu D_s^-}$.
- $\mu^+ D^- (\rightarrow \phi \pi^-)$ signal with fraction $\mathcal{F}_{\mu D^\pm}$.
- $\mu^+ D^- (\rightarrow K \pi \pi^-)$ reflection with fraction $\mathcal{F}_{\mu D_{refl}^\pm}$. The reflection arises due to mass misassignment in this channel. The D^- mass peak shifts to ~ 2 GeV/ c^2 if the kaon mass is incorrectly assigned to one of the pion tracks.

- Combinatorial background with fraction $(1 - \mathcal{F}_{\mu D_s} - \mathcal{F}_{\mu D^\pm} - \mathcal{F}_{\mu D_{refl}^\pm})$.

The fractions $\mathcal{F}_{\mu D_s}$, $\mathcal{F}_{\mu D^\pm}$ and $\mathcal{F}_{\mu D_{refl}^\pm}$ were determined from the mass fit (see Fig. 1). The total probability density function for a B candidate has the form

$$F_n = \mathcal{F}_{\mu D_s} f_{\mu D_s} + \mathcal{F}_{\mu D^\pm} f_{\mu D^\pm} + \mathcal{F}_{\mu D_{refl}^\pm} f_{\mu D_{refl}^\pm} + \left(1 - \mathcal{F}_{\mu D_s} - \mathcal{F}_{\mu D^\pm} - \mathcal{F}_{\mu D_{refl}^\pm}\right) f_{bkg}. \quad (6)$$

The following form was minimized using the MINUIT [15] program:

$$\mathcal{L} = -2 \sum_n \ln F_n, \quad (7)$$

where n varies from 1 to $N_{total\ events}$.

The *pdfs* for the VPDL uncertainty ($P_i^{\sigma_{xM}}$), mass (P_i^m), dilution ($P_i^{d_{pr}}$), and selection variable y (P_i^y) were taken from experimental data. The signal *pdfs* were also used for the $\mu^+ D^- (\rightarrow \phi \pi^-)$ signal and the $\mu^+ D^- (\rightarrow K^+ \pi^- \pi^-)$ reflection. The dependence of the background slope on VPDL was also taken into account. The mass *pdf* for the $\mu^+ D^- (\rightarrow K^+ \pi^- \pi^-)$ reflection was determined from MC. The fraction $\mathcal{F}_{\mu D_{refl}^-}$ of $K^+ \pi^- \pi^-$ reflected events under the $K^+ K^- \pi^-$ curve was determined using a fit to the $M(K^+ K^- \pi^-)$ mass spectrum and was found to be approximately 1% of the number of $\mu^+ D_s^- (\rightarrow \phi \pi^-)$ signal events.

A. *pdf* for $\mu^+ D_s^-$ Signal

The $\mu^+ D_s^-$ sample is composed mostly of B_s^0 mesons with some contribution from B^+ and B_d^0 mesons.

The formulae for the decay rates of neutral B mesons were taken from Ref. [16] and adopted for the flavor-specific case:

$$\Gamma(B^0(t) \rightarrow f) = N_f |A_f|^2 \frac{\exp(-\Gamma t)}{2} \left\{ \cosh\left(\frac{\Delta\Gamma t}{2}\right) + \cos(\Delta M t) \right\} [+ -], \quad (8)$$

$$\Gamma(\bar{B}^0(t) \rightarrow f) = N_f |A_f|^2 (1+a) \frac{\exp(-\Gamma t)}{2} \left\{ \cosh\left(\frac{\Delta\Gamma t}{2}\right) - \cos(\Delta M t) \right\} [++], \quad (9)$$

$$\Gamma(B^0(t) \rightarrow \bar{f}) = N_f |\bar{A}_{\bar{f}}|^2 (1-a) \frac{\exp(-\Gamma t)}{2} \left\{ \cosh\left(\frac{\Delta\Gamma t}{2}\right) - \cos(\Delta M t) \right\} [--], \quad (10)$$

$$\Gamma(\bar{B}^0(t) \rightarrow \bar{f}) = N_f |\bar{A}_{\bar{f}}|^2 \frac{\exp(-\Gamma t)}{2} \left\{ \cosh\left(\frac{\Delta\Gamma t}{2}\right) + \cos(\Delta M t) \right\} [-+]. \quad (11)$$

The parameter $a = a_{sl}^{s(d)}$ is the semileptonic CP asymmetry for the B_s (B_d) meson. The equations above can be modified in the following way to simplify normalization and calculations:

$$\Gamma(B^0(t) \rightarrow f) = N_f |A_f|^2 \frac{1}{2} \left\{ \frac{\exp((- \Gamma - \Delta\Gamma/2)t) + \exp((- \Gamma + \Delta\Gamma/2)t)}{2} + \exp(-\Gamma t) \cos(\Delta M t) \right\}. \quad (12)$$

Assuming no direct CP violation ($|A_f| = |\bar{A}_{\bar{f}}|$), the distribution of the visible proper decay length x for the B_s^0 meson is given by:

$$p_{B_s^0(t) \rightarrow f}(x, K) = \frac{1}{2} \left\{ \frac{\frac{K}{c\tau_{B_s^0 L}} \exp\left(-\frac{Kx}{c\tau_{B_s^0 L}}\right) + \frac{K}{c\tau_{B_s^0 H}} \exp\left(-\frac{Kx}{c\tau_{B_s^0 H}}\right)}{2} + \frac{K}{c\tau_{B_s^0}} \exp\left(-\frac{Kx}{c\tau_{B_s^0}}\right) \cos(\Delta m_s \cdot Kx/c) \right\}, \quad (13)$$

where $\tau_{B_s^0 H} = 1/(\Gamma_s - \Delta\Gamma_s/2)$ and $\tau_{B_s^0 L} = 1/(\Gamma_s + \Delta\Gamma_s/2)$. All the events can be divided into four samples corresponding to the signs of the final and initial state taggings given in square brackets for the equations 8–11. The

dilution of the initial-state tagging leads to the mixture of these samples:

$$p^{+-}(x, K, d_{pr}) = p_{B^0(t) \rightarrow f} \cdot \frac{1 + \mathcal{D}(d_{pr})}{2} + p_{\overline{B}^0(t) \rightarrow f} \cdot \frac{1 - \mathcal{D}(d_{pr})}{2}, \quad (14)$$

$$p^{++}(x, K, d_{pr}) = p_{\overline{B}^0(t) \rightarrow f} \cdot \frac{1 + \mathcal{D}(d_{pr})}{2} + p_{B^0(t) \rightarrow f} \cdot \frac{1 - \mathcal{D}(d_{pr})}{2}, \quad (15)$$

$$p^{-+}(x, K, d_{pr}) = p_{\overline{B}^0(t) \rightarrow \bar{f}} \cdot \frac{1 + \mathcal{D}(d_{pr})}{2} + p_{B^0(t) \rightarrow \bar{f}} \cdot \frac{1 - \mathcal{D}(d_{pr})}{2}, \quad (16)$$

$$p^{--}(x, K, d_{pr}) = p_{B^0(t) \rightarrow \bar{f}} \cdot \frac{1 + \mathcal{D}(d_{pr})}{2} + p_{\overline{B}^0(t) \rightarrow \bar{f}} \cdot \frac{1 - \mathcal{D}(d_{pr})}{2}. \quad (17)$$

Finally, the distribution of visible proper decay length x for corresponding source is

$$p_{VPDL}(x, K, d_{pr}) = \frac{1}{4}(p^{+-} \cdot (1+q_\mu)(1-q_T) + p^{++} \cdot (1+q_\mu)(1+q_T) + p^{-+} \cdot (1-q_\mu)(1+q_T) + p^{--} \cdot (1-q_\mu)(1-q_T)), \quad (18)$$

where q_μ is sign of the muon from B_s decay and q_T is sign of the initial-state tagging determined from the sign of d_{pr} .

The *pdf* 18 should be corrected for the detector charge asymmetries. The corresponding procedure was developed for the previous analyses described in Refs. [3, 5]:

$$p^{q\beta\gamma}(x, K, d_{pr}) = p_{VPDL}(x, K, d_{pr}) \cdot \epsilon^\beta (1 + q_\mu \gamma_\mu A_{fb})(1 + \gamma_\mu A_{det})(1 + q_\mu \beta \gamma_\mu A_{ro})(1 + \beta \gamma_\mu A_{\beta\gamma})(1 + q_\mu \beta A_{q\beta}), \quad (19)$$

where β is the toroid polarity, γ is sign of pseudorapidity ($\gamma = +1$ for $\eta > 0$ and $\gamma = -1$ for $\eta < 0$), q_μ is charge of muon from the B_s decays and ϵ^β is the fraction of events with the toroid polarity $\beta = +1$ or -1 . The parameters A_{fb} , A_{det} , A_{ro} , $A_{\beta\gamma}$ and $A_{q\beta}$ were determined from the fit.

The translation from real VPDL, x , to the measured VPDL, x^M , is achieved by a convolution of the K factors and resolution functions as specified below.

$$P_j^{q\beta\gamma}(x^M, \sigma_{x^M}, d_{pr}) = \int_{K_{min}}^{K_{max}} dK D_j(K) \cdot \frac{Eff_j(x^M)}{N_j(K, \sigma_{x^M}, d_{pr})} \int_0^\infty dx G(x - x^M, \sigma_{x^M}) \cdot p_j^{q\beta\gamma}(x, K, d_{pr}). \quad (20)$$

Here

$$G(x - x^M, \sigma_{x^M}) = \frac{1}{\sqrt{2\pi}\sigma_{x^M}} \exp\left(-\frac{(x - x^M)^2}{2\sigma_{x^M}^2}\right) \quad (21)$$

is the detector resolution of the VPDL and $Eff_j(x)$ is the reconstruction efficiency for a given decay channel j of this type of B meson as a function of VPDL. The function $D_j(K)$ gives the normalized distribution of the K factor in a given channel j . The normalization factor N_j is calculated by integration over the entire VPDL region:

$$N_j(K, \sigma_{x^M}, d_{pr}) = \int_{-\infty}^\infty dx^M Eff_j(x^M) \cdot \int_0^\infty dx G(x - x^M, \sigma_{x^M}) \cdot p_j(x, K, d_{pr}). \quad (22)$$

The total VPDL *pdf* for the $\mu^+ D_s^-$ signal is a sum of all the contributions that yield the D_s^- mass peak:

$$P_{\mu D_s^-}^{q\beta\gamma}(x^M, \sigma_{x^M}, d_{pr}) = (1 - \mathcal{F}_{peak}) \sum_j Br_j \cdot P_j^{q\beta\gamma}(x^M, \sigma_{x^M}, d_{pr}) + \mathcal{F}_{peak} \cdot P_{peak}^{q\beta\gamma}(x^M). \quad (23)$$

Here the sum \sum_j is taken over all decay channels that yield a $\mu^+ D_s^-$ final state and Br_j is the branching rate of a given channel j . In addition to the long-lived $\mu^+ D_s^-$ candidates from B meson decays, there is a contribution, with fraction \mathcal{F}_{peak} , of the ‘‘peaking background’’, which consists of combinations of D_s^- mesons and muons originating from different c or b quarks. The direct c production gives the largest contribution to this background and, therefore, the function $P_{peak}(x^M)$ was determined from $c\bar{c}$ MC. We assume that this background produces negative and positive flavor tags with equal probability.

The branching rates Br_j were taken from the PDG [17], as were the lifetimes of the B_s^0 , B^+ and B_d^0 mesons. The functions $D_j(K)$ and $Eff_j(x)$ were taken from the MC simulation, as explained later.

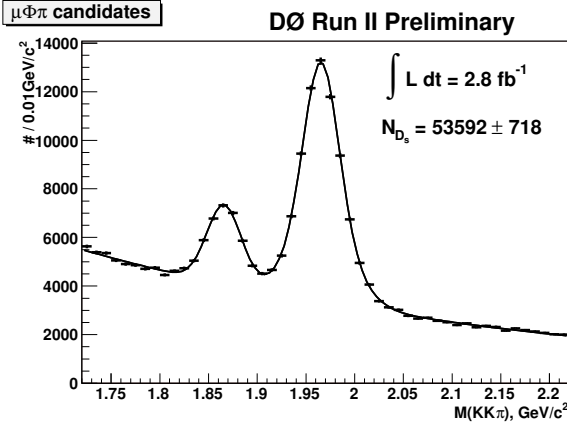


FIG. 1: $M(K^+K^-\pi^-)$ invariant mass distributions for the B_s^0 sample. The left and right peaks correspond to μ^+D^- and $\mu^+D_s^-$ candidates, respectively. The curve represents the fit to this mass spectrum. For fitting the mass spectra, a single Gaussian was used to describe the $D^- \rightarrow \phi\pi^-$ decays and a double Gaussian was used for the $D_s^- \rightarrow \phi\pi^-$ decays. The background is modeled by an exponential.

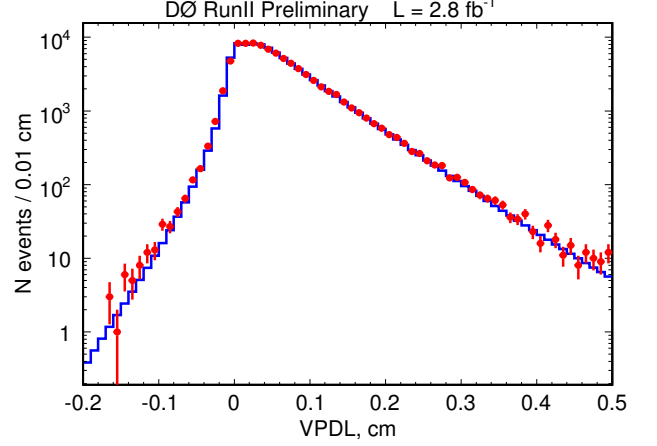


FIG. 2: Distribution of the VPD in the signal region $1.91 < M(D_s^-) < 2.02$ GeV/c^2 . The points represent the experimental data, the histogram shows the fitting function.

B. pdf for Combinatorial Background

The following contributions to the combinatorial background were considered:

1. Background with quasi-vertices distributed around the primary vertex (described as a Gaussian ($G(0 - x^M, \sigma_{peak_bkg})$) with constant width σ_{peak_bkg} ; fraction in the background: \mathcal{F}_{peak_bkg}).
2. Prompt background, with pdf P_{bkg}^{prompt} and with the $\mu^+D_s^-$ vertex coinciding with the primary vertex (described as a Gaussian with a width determined by the resolution; fraction in the background: \mathcal{F}_0). The resolution scale factor for this background is different from the signal resolution scale factor. The scale factor is a free fit parameter, s_{bkg} .
3. Long-lived background, with pdf P_{bkg}^{long} (exponential with constant decay length $c\tau_{bkg}$ convoluted with the resolution). This background was divided into three subsamples:
 - (a) insensitive to the tagging (fraction in the long-lived background: $(1 - \mathcal{F}_{tsens})$);
 - (b) sensitive to the tagging and non-oscillating (fraction in the background sensitive to the tagging: $(1 - \mathcal{F}_{osc})$);
 - (c) sensitive to the tagging and oscillating with frequency Δm_d (fraction in the background sensitive to the tagging: \mathcal{F}_{osc}). The pdf for this background is described by the equations 8–11 with an asymmetry parameter $a = a_{bg}$.

The fractions of these contributions and their parameters were determined from the data sample. The background pdf was expressed in the following form:

$$\begin{aligned}
 P_{bkg}(x^M, \sigma_{x^M}, d_{pr}) &= \mathcal{F}_{peak_bkg} G(0 - x^M, \sigma_{peak_bkg}) + \mathcal{F}_0 P_{bkg}^{prompt}(x^M, \sigma_{x^M}) \\
 &\quad + (1 - \mathcal{F}_{peak_bkg} - \mathcal{F}_0) \cdot P_{bkg}^{long}(x^M, \sigma_{x^M}, d_{pr}), \\
 P_{bkg}^{prompt}(x^M, \sigma_{x^M}) &= \frac{Eff(x^M)}{N} \int_0^\infty dx (G(x - x^M, s_{bkg}\sigma_{x^M})\delta(x)), \\
 P_{bkg}^{long}(x^M, \sigma_{x^M}, d_{pr}) &= \frac{Eff(x^M)}{N} \int_0^\infty dx (G(x - x^M, s_{bkg}\sigma_{x^M}) \cdot p_{bkg}^{long}), \\
 p_{bkg}^{long}(x, d_{pr}) &= \frac{1}{c\tau_{bkg}} \exp\left(-\frac{x}{c\tau_{bkg}}\right) ((1 - \mathcal{F}_{tsens}) + \mathcal{F}_{tsens} ((1 \pm \mathcal{D})(1 - \mathcal{F}_{osc}) + (1 \pm \mathcal{D} \cos(\Delta m_d \cdot x/c)) \cdot \mathcal{F}_{osc})),
 \end{aligned} \tag{24}$$

where N is a normalization constant and the fit parameters include \mathcal{F}_{peak_bkg} , σ_{peak_bkg} , \mathcal{F}_0 , \mathcal{F}_{tsens} , \mathcal{F}_{osc} , $c\tau_{bkg}$ and the efficiency parameters.

The background *pdf* was also corrected for the detector asymmetries.

VII. FIT INPUTS

We have used the following measured parameters for B mesons from the PDG [17] as inputs for the lifetime fitting procedure: $c\tau_{B^+} = 501 \mu\text{m}$, $c\tau_{B_d^0} = 460 \mu\text{m}$, $c\tau_{B_s^0} = 441 \mu\text{m}$, $\Delta\Gamma_{B_s^0} = 0.084 \text{ ps}^{-1}$ and $\Delta m_d = 0.502 \text{ ps}^{-1}$.

A. Sample Composition

The composition of the selected μD_s sample was determined using simulated MC events, taking into account B -meson production rates, the corresponding branching fractions into the μD_s final state, and the reconstruction and trigger turn-on efficiencies for each mode. The following decay channels of the B mesons were considered :

- $B_s^0 \rightarrow \mu^+ \nu D_s^-$;
- $B_s^0 \rightarrow \mu^+ \nu D_s^{*-} \rightarrow \mu^+ \nu D_s^-$;
- $B_s^0 \rightarrow \mu^+ \nu D_{s0}^{*-} \rightarrow \mu^+ \nu D_s^-$;
- $B_s^0 \rightarrow \mu^+ \nu D_{s1}^{\prime-} \rightarrow \mu^+ \nu D_s^-$;
- $B_s^0 \rightarrow \tau^+ \nu D_s^- X, \tau \rightarrow \mu \nu \nu$;
- $B_s^0 \rightarrow D_s^+ D_s^- X; D_s^- \rightarrow \mu \nu X$;
- $B_s^0 \rightarrow D_s D X; D \rightarrow \mu \nu X$;
- $B^+ \rightarrow D D_s^- X; D \rightarrow \mu \nu X$;
- $B^0 \rightarrow D D_s^- X; D \rightarrow \mu \nu X$;

The latest PDG values were used to determine the branching fractions of decays contributing to the D_s^- sample. For those branching fractions not given in the PDG, we used the values provided by EvtGen [18], which are motivated by theoretical considerations.

Taking into account the corresponding branching rates and reconstruction efficiencies, we calculated the contributions to our signal region from the various processes. The $B_s^0 \rightarrow D_s^- \mu^+ \nu X$ modes (including feed-down via D_s^{*-} , D_{s0}^{*-} , and $D_{s1}^{\prime-}$ decays and muons originating from τ decays) comprise $(91.0 \pm 3.3)\%$ of our sample, after accounting for reconstruction efficiencies. In addition, $B \rightarrow D_{(s)}^+ D_s^- X$ decays followed by $D_{(s)}^+ \rightarrow \mu^+ \nu X$ include both a real D_s^- and μ^+ and yield a mass in the signal region but are not expected to oscillate with Δm_s . The assigned uncertainty to each channel covers possible trigger efficiency biases.

In determining the K factor distributions, MC generator-level information was used for the computation of p_T . Following the definition used in Eq. 4, the K factor distributions for all considered decays were determined [20]. The K factors for D_s^{*-} , D_{s0}^{*-} and $D_{s1}^{\prime-}$ have lower mean values because more decay products are lost. Since the K factors in Eq. 4 were defined as the ratio of transverse momenta, they can exceed unity. The K factors are binned in ten $D_s \mu$ mass bins, motivated by the narrowing of the K factor distributions with increasing $D_s \mu$ mass. In addition, the muon trigger turn-on curves [21] are applied to take into account trigger effects that sculpt the K factor distributions.

The VPDL uncertainty was estimated by the vertex fitting procedure. A resolution scale factor, determined using a J/ψ data sample, was introduced to take into account a possible bias. The negative tail of the pull distribution of the J/ψ vertex position with respect to that of the primary vertex should be a Gaussian with a sigma of unity if uncertainties assigned to the vertex coordinates are correct. We ignore the positive side of the pull distribution as that tends to be biased towards larger values due to J/ψ mesons from real B meson decays. For this study we exclude muons from J/ψ decays from the primary vertex. The resulting pull distribution was fitted using a double Gaussian.

VIII. RESULTS

Lifetime fit

The efficiency curves for the decay modes contributing to the signal peak were taken from MC. To take into account possible discrepancies between data and MC due to trigger requirements, the efficiency curve for $B_s \rightarrow X\mu D_s^-$ was tuned using the full data sample after fixing the B_s^0 lifetime to its PDG value and releasing the efficiency parameters in the likelihood fit.

The contribution of the peaking (prompt) background from direct $c\bar{c}$ production was estimated to be 8.8% [22]. The lifetime fits for the signal region are shown in Fig. 2.

Asymmetry fits

Combinatorial background

Asymmetries in the combinatorial background were determined from the sidebands. All the asymmetries except A_{ro} have fit values close to zero.

Signal

As expected, the detector asymmetries were found to be similar for the signal and background. The value of B_s oscillation frequency was fixed at $\Delta m_s = 17.77\text{ps}^{-1}$ [23] in the fit. Table I shows the asymmetries for the combined data sample.

TABLE I: Asymmetry parameters. The quoted uncertainties are statistical.

Parameter	RunII, $\int Ldt = 2.8 \text{ fb}^{-1}$
a_{sl}^s	-0.0024 ± 0.0117
a_{sl}^d	-0.0787 ± 0.0371
a_{bg}	-0.0182 ± 0.0271
A_{fb}	0.0000 ± 0.0021
A_{det}	0.0001 ± 0.0021
A_{ro}	-0.0323 ± 0.0021
$A_{\beta\gamma}$	-0.0005 ± 0.0021
$A_{q\beta}$	0.0029 ± 0.0021

IX. SYSTEMATIC UNCERTAINTIES

The largest contribution to the systematic uncertainty is due to the efficiency curve. It was estimated by comparing the results obtained with the efficiency curves from MC ($a_{sl}^s = -0.0048 \pm 0.0117$) and the default ones. The second largest contribution to the systematic uncertainty is due to $c\bar{c}$ background. Its contribution was varied to 11.8% [22] and the asymmetry result changed to $a_{sl}^s = -0.0010 \pm 0.0119$. The contribution to the systematic uncertainty due to mass fitting procedure is $\Delta_{mass} = +0.0004$. The uncertainty of total branching fraction of $B_s^0 \rightarrow D_s^{(*)}\mu\nu$ decay contributes $\Delta_{B_s^0 \rightarrow D_s^{(*)}\mu\nu} = -0.0003$.

A set of K factor distributions scaled up/down by 2% were utilized to account for the lack of knowledge in the relative branching fractions of the $B_s^0 \rightarrow D_s^{(*)}\mu\nu$ decay, for which no measurements exist. Monte Carlo studies indicate that a 2% variation is sufficient to account for shifts in the means of the K factor distributions for extreme variations in the relative branching fractions [20]. Their contributions to the systematic uncertainty are negligible in comparison with the ones mentioned above.

The final result, including systematic uncertainties, is $a_{sl}^s = -0.0024 \pm 0.0117(stat)_{-0.0024}^{+0.0015}(syst)$.

X. CONCLUSIONS

Using $B_s^0 \rightarrow D_s^- \mu^+ \nu X$ decay sequence $D_s^- \rightarrow \phi \pi^-$, $\phi \rightarrow K^+ K^-$, in combination with initial-state flavor tagging and an unbinned fit, we measured the asymmetry in semileptonic B_s decays to be $a_{sl}^s = -0.0024 \pm 0.0117(stat)_{-0.0024}^{+0.0015}(syst)$. This is the most precise direct measurement of this asymmetry to date. This result supersedes the DØ result without initial-state flavor tagging [5]. It can be combined with the result of the inclusive di-muon analysis [3] because the overlap between these samples is small (see the combination paper [24]). As the result is statistics limited, an improved measurement will be available as DØ collects additional data.

- [1] V. Abazov *et al.* [DØ Collaboration], arXiv:0802.2255 [hep-ex].
- [2] T. Aaltonen *et al.* [CDF Collaboration], arXiv:0712.2397 [hep-ex].
- [3] V. Abazov *et al.* [DØ Collaboration], Phys. Rev. D **74**, 092001 (2006) [arXiv:hep-ex/0609014].
- [4] CDF Collaboration, CDF note 9015.
- [5] V. Abazov *et al.* [DØ Collaboration], Phys. Rev. Lett. **98**, 151801 (2007) [hep-ex/0701007].
- [6] V. Abazov *et al.* [DØ Collaboration], Phys. Rev. Lett. **97**, 021802 (2006) [hep-ex/0603029].
- [7] V. Abazov *et al.* [DØ Collaboration] *The Upgraded DØ Detector*, Nucl. Instrum. Meth. A **565**, 463 (2006).
- [8] V. M. Abazov *et al.*, Nucl. Instrum. Meth. A **552**, 372 (2005).
- [9] V. Abazov *et al.* [DØ Collaboration], Phys. Rev. D **74**, 112002 (2006) [arXiv:hep-ex/0609034].
- [10] G. Borisov, A. Rakitin, “Flavor Tagging Technique for B_s Mesons”, DØ note 5210, July 2006.
- [11] S. Catani, Yu.L. Dokshitzer, M. Olsson, G. Turnock, B.R. Webber, Phys. Lett. **B269** (1991) 432.
- [12] T. Sjöstrand *et al.*, hep-ph/0108264.
- [13] DELPHI Collab., *b-tagging in DELPHI at LEP*, Eur. Phys. J. **C32** (2004), 185-208.
- [14] G. Borisov, Nucl. Instrum. Meth. A **417**, 384 (1998).
- [15] F. James, *MINUIT - Function Minimization and Error Analysis*, CERN Program Library Long Writeup D506, 1998.
- [16] K. Anikeev *et al.*, *B Physics at the Tevatron: Run II and Beyond*, Fermilab-Pub-01-197 (2001); hep-ph/0201071.
- [17] S. Eidelman *et al.*, Phys. Lett. **B592**, 1 (2004).
- [18] D.J. Lange, Nucl. Instrum. Meth. A **462**, 152 (2001); for details see <http://www.slac.stanford.edu/~lange/EvtGen>.
- [19] E. Barberio *et al.* [Heavy Flavor Averaging Group], “Averages of b-hadron properties at the end of 2006”, [arXiv:hep-ex/0704.3575], Page 41, Table 18.
- [20] J. Radigan and W. Taylor, “The K Factor in Semileptonic B_s Decays in the $D_s \rightarrow \phi \pi$ Decay Mode”, DØ note 5221, August 2006.
- [21] S. Youn, B. Casey, D. Buchholz and D. Tsybychev, “Trigger Efficiency Study for Run II at D0 using Inclusive Muon Sample”, DØ note 5522, October 2007.
- [22] C. Ay *et al.*, “Study of $c\bar{c}$ contribution to the semileptonic sample of B mesons” DØ note 4639.
- [23] A. Abulencia *et al.* [CDF Collaboration], Phys. Rev. Lett. **97**, 242003 (2006).
- [24] V. Abazov *et al.* [DØ Collaboration], Phys. Rev. D **76**, 057101 (2007). [hep-ex/0702030].